Available online at www.sciencedirect.com
ScienceDirect
Optics Communications 271 (2007) 48–58
OPTICS COMMUNICATIONS
www.elsevier.com/locate/optcom

Effects of threshold on single-target detection by using modified amplitude-modulated joint transform correlator

Pitchaya Kaewkasi [a], Joewono Widjaja [a,*], Jun Uozumi [b]

[a] *Institute of Science, Suranaree University of Technology, Nakhon Ratchasima 30000, Thailand*
[b] *Faculty of Engineering, Hokkai-Gakuen University, Sapporo 064-0926, Japan*

Received 13 December 2005; received in revised form 27 September 2006; accepted 5 October 2006

Abstract

Effects of threshold value on detection performance of the modified amplitude-modulated joint transform correlator are quantitatively studied using computer simulation. Fingerprint and human face images are used as test scenes in the presence of noise and a contrast difference. Simulation results demonstrate that this correlator improves detection performance for both types of image used, but moreso for human face images. Optimal detection of low-contrast human face images obscured by strong noise can be obtained by selecting an appropriate threshold value.

Keywords: Target detection; Modified amplitude-modulated joint transform correlator; Detection performance

1. Introduction

In recent years, much research has been devoted to joint transform correlator (JTC) for implementing real-time optical pattern recognition [1–3]. The reason for this interest is that unlike VaderLugt correlator synthesis of complex matched filters is not necessary. By taking this advantage into account, real-time implementation of the JTC can be accomplished by using spatial light modulator (SLM) together with charge-coupled device (CCD) sensor. However, the implementation of the JTC still suffers from several limitations such that its correlation output contains a strong zero-order peak with broad correlation width and that its discrimination ability is low [1–5]. These problems cause difficulties in correctly identifying objects in automatic target detections. Therefore, there are many interests to improve the detection performance of the JTC.

Amplitude-modulated JTC (AMJTC) [6] is one of several approaches to eliminate the limitations of the classical JTC by multiplying a joint power spectrum (JPS) with an amplitude-modulated filter (AMF) whose transfer function is determined by thresholding the power spectrum of the reference image. Although this method produces a better correlation result than the classical JTC, it is not tolerant to the presence of noise. Consequently, Huang et al. [3] introduced a method for improving the performance of the AMJTC which is called the modified AMJTC. This method is performed by subtracting the power spectra of the reference and of the target images from the JPS before multiplying with the AMF. The correlation performance of this approach is enhanced to be better than other JTC approaches. Although the effectiveness of the modified AMJTC depends on the selected threshold value of the AMF, the criteria to select the appropriate threshold for the AMF have not been fully investigated. Accordingly, in this paper the effects of the threshold on detection of single target by using the modified AMJTC are quantitatively studied. In this study, two types of images with different spatial frequency contents are used as test scenes in the presence of noise in the input plane and a contrast difference between the target and the reference images that may arise from unbalanced illumination. For the purpose of investigating the result of this work, the computer

* Corresponding author. Tel.: +66 44224194; fax: +66 44224185.
E-mail address: widjaja@sut.ac.th (J. Widjaja).

0030-4018/$ - see front matter © 2006 Elsevier B.V. All rights reserved.
doi:10.1016/j.optcom.2006.10.002

simulation is used to present the result. This paper is organized as follows. The theoretical discussion of the modified AMJTC is described in Section 2. Section 3 provides the discussion of the computer simulation result of modified AMJTC on single-target detection. Finally, the conclusions are presented in the last section.

2. Theoretical background

Fig. 1 illustrates a schematic diagram of an optical setup for implementing the real-time modified AMJTC. The architecture of this setup is based on an optical Fourier transform where an electronically addressed SLM (EASLM) placed in the front focal plane of the Fourier transforming lens L1 is used to display an input image to be processed, while the CCD1 placed at the back focal plane of the lens is used to capture its Fourier transformed output. In this setup, a set of reference images and their corresponding power spectra are prepared and stored into a computer system prior to detection. The power spectrum is optically generated by taking Fourier transform of the reference image displayed onto the EASLM. The generated power spectrum at the back focal plane of the lens is captured by the CCD1 and stored into the computer system. In order to detect the target image $t(x,y)$, the input scene is captured by using the CCD2. After storing the captured target image into the computer, its power spectrum is generated and stored in the same way as the reference image. Subsequently, the reference $r(x,y)$ and the target $t(x,y)$ are displayed side-by-side on the EASLM with a separation of $2x_0$ to form a joint input image, which can be mathematically expressed as

$$f(x,y) = r(x-x_0,y) + t(x+x_0,y). \tag{1}$$

When the input target image is corrupted by an additive Gaussian noise $n(x,y)$ and the contrast of the reference and the target images is different, the joint input image can be rewritten as

$$f(x,y) = r(x-x_0,y) + c_{\mathrm{T}}t(x+x_0,y) + n(x+x_0,y), \tag{2}$$

where c_{T} is the ratio of the amplitude of the target image to the reference image. The factor c_{T} is greater than, equal to, or smaller than 1 when the contrast of the reference image is lower than, equal to, or higher than that of the target, respectively [7].

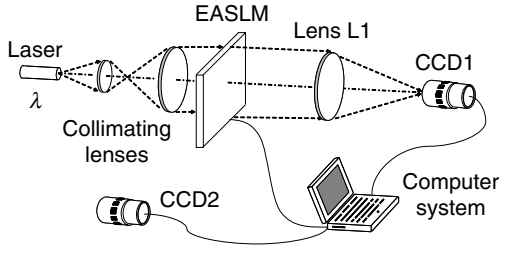

Fig. 1. Schematic diagram of optical setup for implementing real-time modified AMJTC.

By illuminating perpendicularly the EASLM placed in the front focal plane of a lens L1 with a coherent plane wave, the joint Fourier spectrum appears at the back focal plane of the lens L1. Capturing the intensity of this spectrum by using CCD1 yields the JPS which is mathematically given by

$$\begin{aligned}|F(f_x,f_y)|^2 &= |R(f_x,f_y)|^2 + c_{\mathrm{T}}^2|T(f_x,f_y)|^2 + |N(f_x,f_y)|^2 \\ &\quad + c_{\mathrm{T}}[T^*(f_x,f_y)N(f_x,f_y) + T(f_x,f_y)N^*(f_x,f_y)] \\ &\quad + c_{\mathrm{T}}[R(f_x,f_y)T^*(f_x,f_y)\exp(-\mathrm{j}4\pi f_x x_0) \\ &\quad + T(f_x,f_y)R^*(f_x,f_y)\exp(\mathrm{j}4\pi f_x x_0)] \\ &\quad + R(f_x,f_y)N^*(f_x,f_y)\exp(-\mathrm{j}4\pi f_x x_0) \\ &\quad + N(f_x,f_y)R^*(f_x,f_y)\exp(\mathrm{j}4\pi f_x x_0).\end{aligned} \tag{3}$$

Here, $R(f_x,f_y)$, $T(f_x,f_y)$ and $N(f_x,f_y)$ are the Fourier transforms of the reference, the target and the noise, respectively. f_x and f_y stand for the spatial frequency coordinates in the x and the y directions, respectively, at the Fourier plane. To overcome the problems of a complicated strong zero-order term and the noise terms, the power spectra of the reference and of the noise-corrupted input target that correspond to the first five terms of Eq. (3) are digitally subtracted from Eq. (3) by computer [3]. The subtraction gives

$$\begin{aligned}U(f_x,f_y) &= |F(f_x,f_y)|^2 - \{|R(f_x,f_y)|^2 + c_{\mathrm{T}}^2|T(f_x,f_y)|^2 \\ &\quad + |N(f_x,f_y)|^2 + c_{\mathrm{T}}[T^*(f_x,f_y)N(f_x,f_y) \\ &\quad + T(f_x,f_y)N^*(f_x,f_y)]\} \\ &= c_{\mathrm{T}}[R(f_x,f_y)T^*(f_x,f_y)\exp(-\mathrm{j}4\pi f_x x_0) \\ &\quad + T(f_x,f_y)R^*(f_x,f_y)\exp(\mathrm{j}4\pi f_x x_0)] \\ &\quad + R(f_x,f_y)N^*(f_x,f_y)\exp(-\mathrm{j}4\pi f_x x_0) \\ &\quad + N(f_x,f_y)R^*(f_x,f_y)\exp(\mathrm{j}4\pi f_x x_0).\end{aligned} \tag{4}$$

As can be seen from Eq. (4), the dc and some noise terms are eliminated. To enhance the performance of the system, the resultant JPS is modulated by the AMF defined as [3]

$$H_{\mathrm{AMF}}(f_x,f_y) = \begin{cases} \mathrm{TH}/|R(f_x,f_y)|^2 & \text{when } |R(f_x,f_y)|^2 \geqslant \mathrm{TH} \\ 1 & \text{when } |R(f_x,f_y)|^2 < \mathrm{TH}, \end{cases} \tag{5}$$

where TH is the threshold value used to determine the transfer function of the AMF. Since for a given threshold value TH the second condition of Eq. (5) can be satisfied by several frequency components of the reference image, the synthesized AMF may contain several cutoff frequencies. Therefore, the transfer function of the AMF is not a smooth function. Below the cutoff frequency, the frequency component of the input signal is attenuated by a factor $\mathrm{TH}/|R(f_x,f_y)|^2$, while the higher ones will not be affected. In comparison with low threshold value, the AMF synthesized by using high threshold value attenuates narrow band of low frequency components around the dc frequency. When the threshold value becomes lower, the attenuation extends to wider band of frequency components. Therefore, for a low threshold, only high frequency components

can pass the filter without attenuation. The modified amplitude modulated JPS can be mathematically rewritten as

$$\begin{aligned} &H_{\mathrm{AMF}}(f_x,f_y)U(f_x,f_y)\\ &\quad= H_{\mathrm{AMF}}(f_x,f_y)\{c_{\mathrm{T}}[R(f_x,f_y)T^*(f_x,f_y)\exp(-\mathrm{j}4\pi f_x x_0)\\ &\qquad+ T(f_x,f_y)R^*(f_x,f_y)\exp(\mathrm{j}4\pi f_x x_0)]\\ &\qquad+ R(f_x,f_y)N^*(f_x,f_y)\exp(-\mathrm{j}4\pi f_x x_0)\\ &\qquad+ N(f_x,f_y)R^*(f_x,f_y)\exp(\mathrm{j}4\pi f_x x_0)\}. \end{aligned} \tag{6}$$

By taking the property of the AMF into account, Eq. (6) can be mathematically regarded as a process of attenuating the spectrum components of the modified JPS below the cutoff frequency of the AMF by the factor $\mathrm{TH}/|R(f_x,f_y)|^2$. Since higher frequency spectrum is not affected, this is equivalent to an edge enhancement process. By displaying the modified JPS into the EASLM, its optical Fourier transform produces the correlation output, called the modified AMJTC, at the back focal plane of the lens L1 as

$$\begin{aligned} c(x,y) &= F^{-1}\{H_{\mathrm{AMF}}(f_x,f_y)U(f_x,f_y)\}\\ &= c_{\mathrm{T}}h_{\mathrm{AMF}}(x,y)\otimes r(x,y) * t(x,y)\otimes\{\delta(x-2x_0,y)\\ &\quad+\delta(x+2x_0,y)\}+h_{\mathrm{AMF}}(x,y)\otimes r(x,y) * n(x,y)\\ &\quad\otimes\{\delta(x-2x_0,y)+\delta(x+2x_0,y)\}, \end{aligned} \tag{7}$$

where $\otimes$, $*$ and F^{-1} denote the convolution, the correlation and the inverse Fourier transform operators, respectively. $h_{\mathrm{AMF}}(x,y)$ corresponds to the impulse response of the AMF. Besides being scaled by the contrast ratio, the first term of Eq. (7) is the correlation between the reference and the target, while the second term of Eq. (7) is the correlation between the reference and the noise. Both terms are convolved with the impulse response of the AMF $h_{\mathrm{AMF}}(x,y)$. These pairs of correlation appear at the position $\pm 2x_0$. When the threshold value of the AMF is properly selected, the noise will be lowered and the correlation width is sharpened.

3. Computer simulation

To investigate the effects of threshold on single-target detection by using the modified AMJTC, the fingerprint and the human face images were used as the test scenes having high- and low-spatial-frequency contents. They consisted of 124×186 pixels with 8-bit gray levels. Fig. 2a and b show the high-contrast test scenes, while their low-contrast images are illustrated in Fig. 2c and d. Note that measurements of the contrast of the two images by using the contrast function can be found in our previous work [7]. The averages of the contrast function were calculated and are 0.28×10^{-2} and 0.11×10^{-2} for Fig. 2a and b, respectively, while they are 0.29×10^{-3} and 0.70×10^{-3} for Fig. 2c and d, respectively. In our study, the joint input image was constructed by separating the reference and the target images with a distance $2x_0 = 248$ pixels in the area of 832×624 pixels. The simulation was performed by using Matlab 6.0 run on a Windows-based personal computer. The FFT2 and the IMNOISE commands were used to calculate the two-dimensional Fourier spectrum of the images and to add the Gaussian noise to an image, respectively. After digital subtraction of the power spectra of the reference and of the target images that were stored in the computer, the modified JPS was then digitally multiplied with the AMF that was generated by a computer in the following steps:

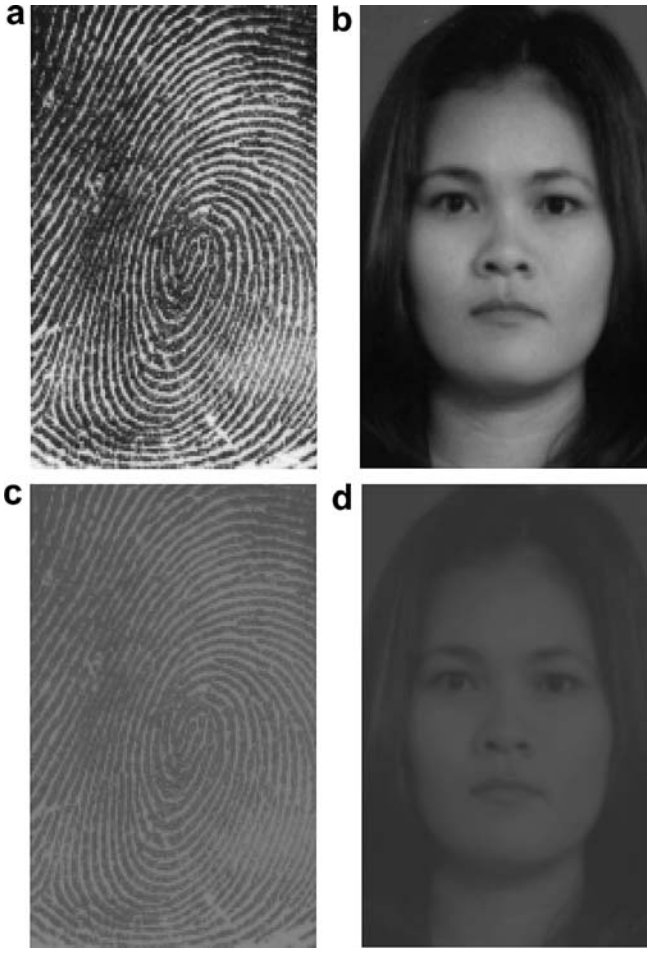

Fig. 2. Test images: (a) high-contrast fingerprint, (b) high-contrast human face, (c) low-contrast fingerprint and (d) low-contrast human face.

- A moving average of the power spectrum of the reference image is computed.
- From the averaged spectrum, several points separated by equal interval are selected between the zero and the highest spatial frequencies along one of the axis of the power spectrum. In our study, we used 8 points between the zero and the highest spatial frequencies of the image.
- The value of the power spectrum at each selected point was used as the threshold value to generate the corresponding AMF.

In order to obtain results applicable to more general images, the threshold value is related to the percentage number of pixels of the power spectrum having value less than the threshold defined as

$$N = \frac{\text{Number of pixels with value less than the threshold value}}{\text{Total number of pixels of the power spectrum}}. \tag{8}$$

According to Eq. (5), the pixels of the power spectrum with value less than the selected threshold value correspond to the pixel of the AMF having a unit amplitude. Hence, Eq. (8) can be rewritten as

$$N = \frac{\text{Number of pixels of the AMF with value 1}}{\text{Total number of pixels of the AMF}}. \tag{9}$$

Since, high and low values of the percentage N can be associated with the AMF generated by using high and low threshold values, respectively, the percentage N represents the extent of attenuation of the modified JPS. When the percentage N is high, the attenuation occurs in narrow band of low-spatial frequencies, while lower value affects wider band of spatial frequencies.

By calculating the inverse Fourier transform of the product of the modified JPS and the AMF, and then taking the square modulus of the result, the correlation peak intensity was obtained as the final result. The ratio of the correlation peak to the correlation deviation (PCD) defined as [8]

$$\text{PCD} = \frac{I(i,j)_{\max}}{\left\{\frac{1}{K\times L}\sum_{i=0}^{K-1}\sum_{j=0}^{L-1}[I(i,j) - E\{I(i,j)\}]^2\right\}^{1/2}} \tag{10}$$

was used to measure the quality of the correlation output. $I(i,j)$ is the maximum intensity of the correlation output and $E\{I(i,j)\}$ is the mean of the correlation intensity. When the target matches with the reference the PCD of Eq. (10) is large, because the correlation output is sharp and its standard deviation is small. However, when the target does not match with the reference, the PCD is small because the correlation output is broad and its standard deviation is large. In order to compare with the detection performance of the classical JTC, the PCD obtained from the modified AMJTC was normalized by the PCD of the classical JTC. It is expected that the normalized PCD will be greater than 1, because the performance of the modified AMJTC is better than that of the classical JTC. The quality of the correlation output is also measured by the full area at half maximum (FAHM).

3.1. High-contrast fingerprint as the reference image

The 3D plots of the autocorrelation of the noise-free high-contrast fingerprints which were pre-processed by using the AMF with $N = 64.7\%$ that corresponds to low threshold and $N = 99.8\%$ that corresponds to high threshold are shown in Fig. 3a and b, respectively. Their correlation peaks are sharp with the FAHMs always equal to 1×1 pixel. However, it can be seen that the correlation peak intensity of Fig. 3a is about two orders of magnitude lower than that of Fig. 3b, because the AMF with low threshold value eliminates the low-spatial-frequency components of the JPS. Since most energy of the signal concentrates on low-frequency components, this elimination reduces the correlation peak. In contrast, besides producing high corre-

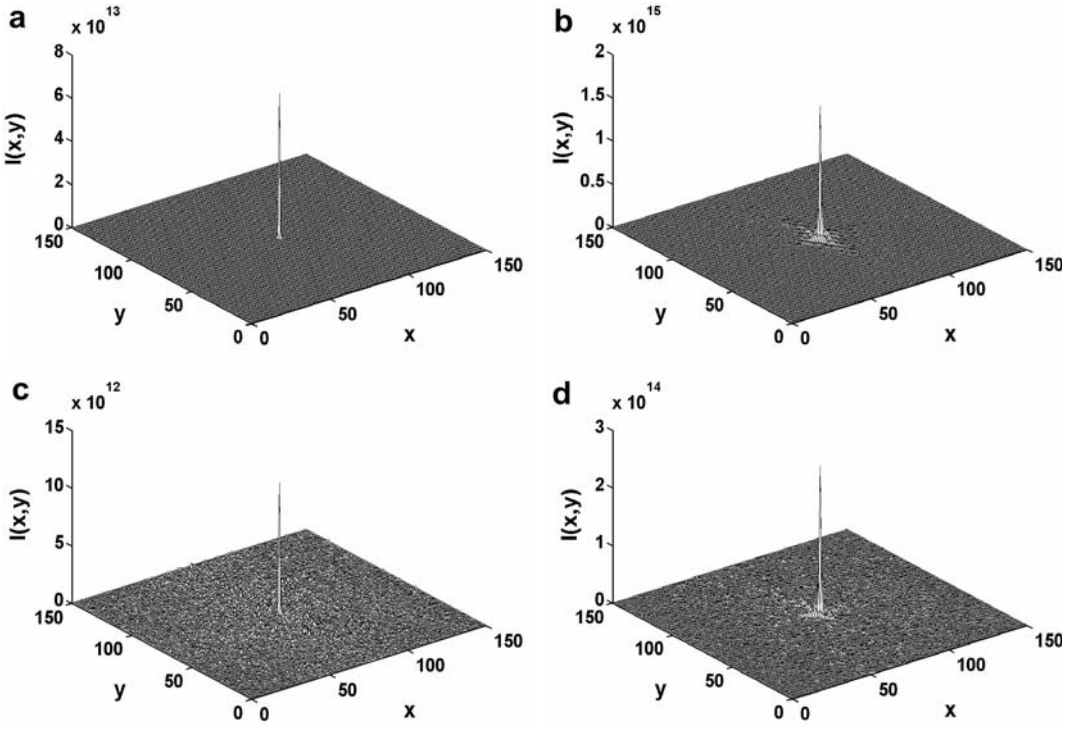

Fig. 3. Autocorrelation outputs of noise-free high-contrast fingerprint pre-processed by the AMF with (a) $N = 64.7\%$ and (b) $N = 99.8\%$. Cross-correlation outputs of noise-free high-contrast fingerprint reference and noisy high-contrast fingerprint target pre-processed by the AMF with (c) $N = 64.7\%$ and (d) $N = 99.8\%$.

lation peak the pre-processing by the AMF with high threshold causes the correlation plane to be noisy. This is because this AMF attenuates less low-frequency components of the JPS than that with low threshold.

Fig. 3c and d show the 3D plots of the correlation outputs of the noisy high-contrast fingerprint with noise variance $\sigma^2 = 1$ pre-processed by using the AMF with $N = 64.7\%$ and $N = 99.8\%$, respectively. This variance value corresponds to strong noise level which was used in our previous work [7]. It is obvious that the desired correlation peaks are still sharp with the FAHMs of 1×1 pixel. In comparison with Fig. 3a and b, the presence of noise in the input plane causes simultaneously the decrease in the peak intensities by about one order of magnitude and the increase in noise in the correlation plane. Since the spectrum of the noise extends over the entire frequency domain, however, the use of the AMF with low threshold cannot reduce totally the noise. As a result, the noise in the correlation plane and the peak intensity of Fig. 3d are higher than those of Fig. 3c.

The correlation outputs of the modified AMJTC of the noise-free low-contrast fingerprint target pre-processed by the AMF with $N = 64.7\%$ and $N = 99.8\%$ are plotted in Fig. 4a and b, respectively. In comparison with Fig. 3a and b, similar correlation outputs with lower peaks are obtained, because the contrast ratio c_T, which is smaller than 1, reduces the output of the first correlation term of Eq. (7). The correlation outputs of the noise-corrupted low-contrast fingerprint targets pre-processed with $N = 64.7\%$ and $N = 99.8\%$ are shown in Fig. 4c and d, respectively. The further decrease in the correlation peaks and the increase in noise in the correlation plane are caused by the noise, which is stronger than the luminance of the low-contrast fingerprint target [7,9]. As a consequence, the first correlation term of Eq. (7) is smaller than the second term. Thus with the same noise level, Fig. 3c and d contain higher correlation peaks.

Fig. 5 shows the variation of the normalized PCDs as a function of the percentage N for different targets detected by using high-contrast fingerprint reference. The normalized PCDs of the noise-free high- and low-contrast fingerprint targets coincide, because scaling of the first correlation term of Eq. (7) by the contrast ratio affects both the correlation peak and the standard deviation of the correlation intensity. It is obvious that when the percentage N reduces, the normalized PCDs increase gradually. This occurs because at high percentage N the AMF attenuates less low-spatial-frequency components than that at low percentage. As a consequence the standard deviation of the correlation intensities at high percentage N is much higher than that at low N. Therefore, the normalized PCD at small percentage N is higher than that at high percentage.

As can be seen in Figs. 3 and 4, when the input targets are corrupted by strong noise such as with variance $\sigma^2 = 1$, the desired correlation peak decreases and the noise in the correlation plane increases. It is found that the standard deviation of the correlation intensities is always lower

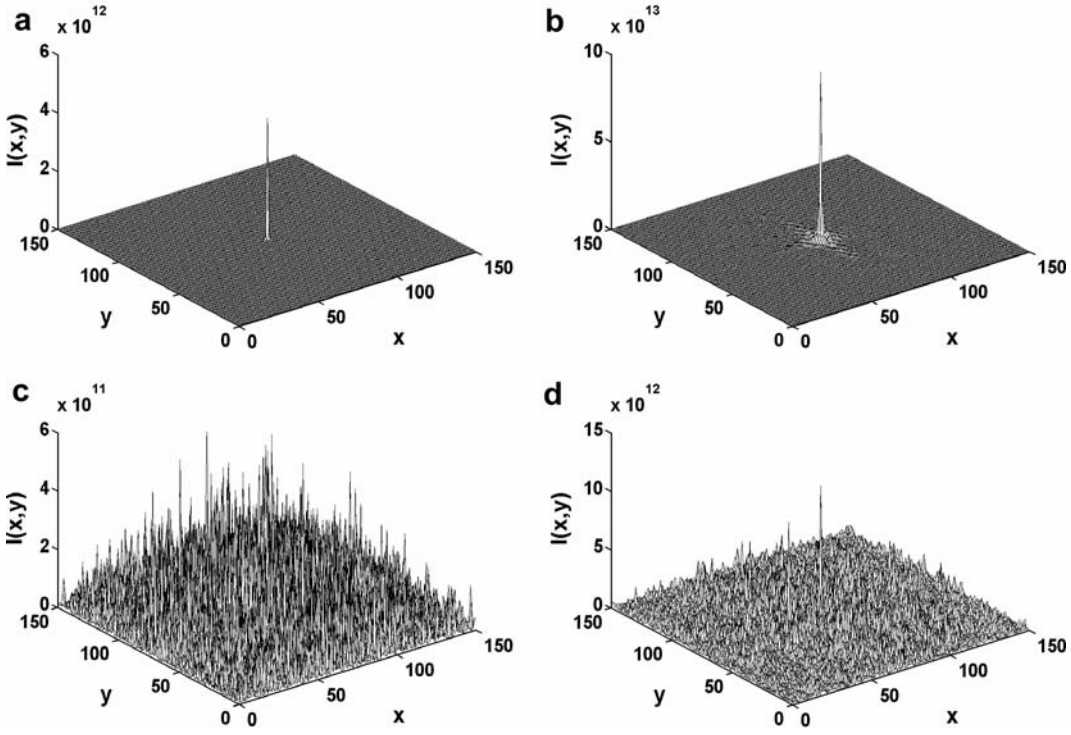

Fig. 4. Cross-correlation outputs of noise-free high-contrast fingerprint reference and noise-free low-contrast fingerprint target pre-processed by the AMF with (a) $N = 64.7\%$ and (b) $N = 99.8\%$. Cross-correlation outputs of noise-free high-contrast fingerprint reference and noisy low-contrast fingerprint target pre-processed by the AMF with (c) $N = 64.7\%$ and (d) $N = 99.8\%$.

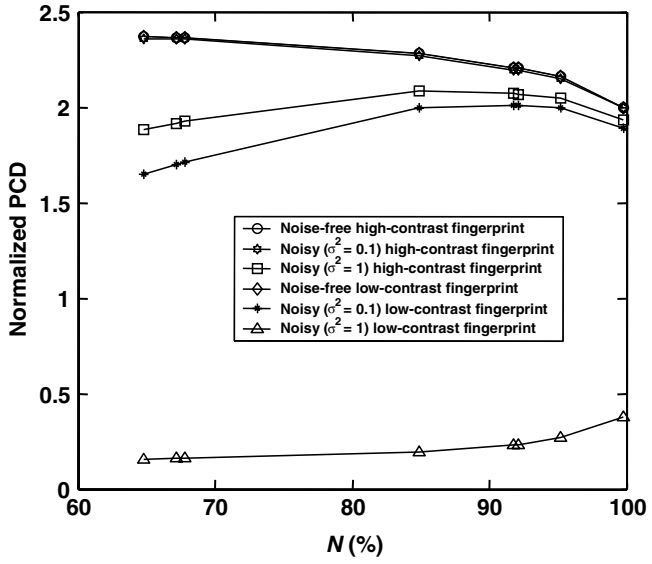

Fig. 5. The normalized PCD as a function of the percentage N of high-contrast fingerprint reference.

than the correlation peak regardless of the threshold values. As the percentage N reduces the standard deviation decreases at a slower rate compared to the decrease of the correlation peak. This is because the noise cannot be totally eliminated by the AMF with low percentage N. For this reason, the normalized PCD of the detection of the noisy high-contrast fingerprint at low percentage N is lower than that at high percentage.

Unlike the noisy high-contrast fingerprint, in the detection of the noisy low-contrast target the modified AMJTC is not robust to noise. As the variance of the noise increases to 1, the normalized PCD reduces sharply to less than 0.4. As shown in Fig. 4c and d, this is mainly caused by the decrease in the first correlation term of Eq. (7) and the presence of noise. As the threshold value becomes higher, the desired correlation peak increases. Consequently, the normalized PCD at high percentage N is slightly higher than that at low percentage. Therefore, the detection of the low-contrast fingerprint target by the modified AMJTC depends on the noise level in the input plane. In the case of the presence of strong noise, the detection of the low-contrast target may not be accomplished. In order to obtain high normalized PCDs, the detection of the noise-free target should be done by using the AMF with low threshold while, for the detection of the noisy high-contrast fingerprint target, the threshold value should be high.

3.2. Low-contrast fingerprint as the reference image

Fig. 6a and b show the 3D autocorrelation outputs of the noise-free low-contrast fingerprint targets pre-processed by using the AMF with $N = 64.7\%$ that corresponds to low threshold and $N = 99.8\%$ that corresponds to high threshold, respectively. In comparison with Fig. 3a and b, the results are similar in that the autocorrelation width of the low-contrast fingerprint detection is as sharp as that of the high-contrast fingerprint. Due to the low contrast

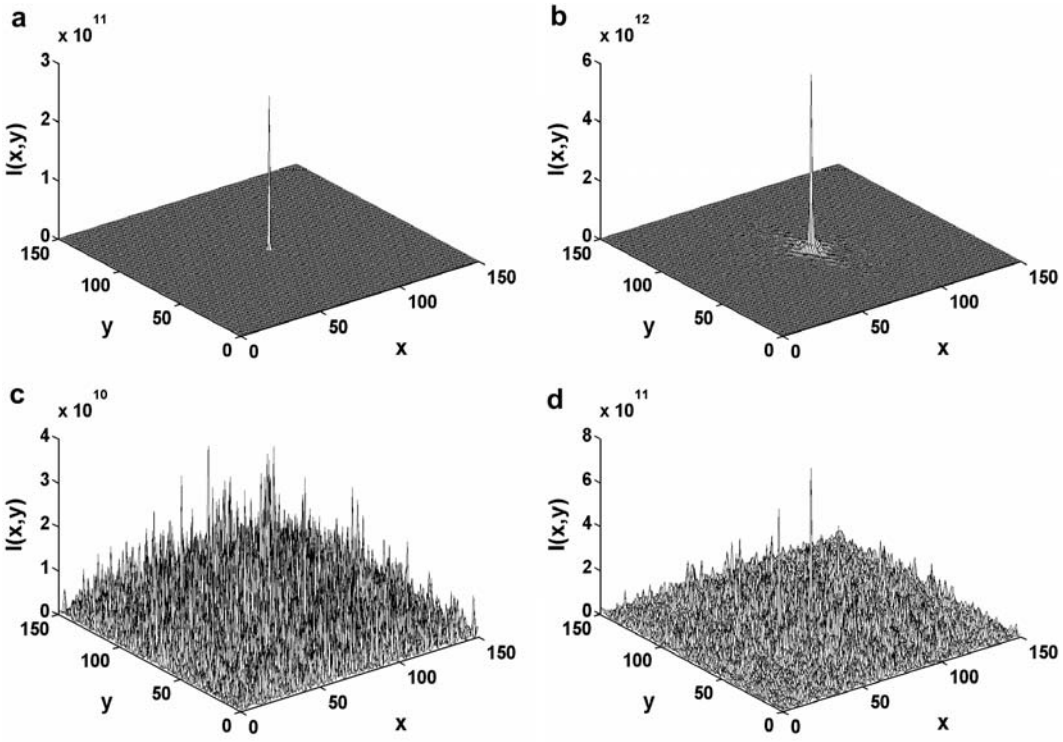

Fig. 6. Autocorrelation outputs of noise-free low-contrast fingerprint pre-processed by the AMF with (a) $N = 64.7\%$ and (b) $N = 99.8\%$. Cross-correlation outputs of noise-free low-contrast fingerprint reference and noisy low-contrast fingerprint target pre-processed by the AMF with (c) $N = 64.7\%$ and (d) $N = 99.8\%$.

of the image, however the correlation peak intensities are reduced by about two orders of magnitude. At high threshold value of the AMF, the correlation plane also appears to be noisy. The correlation outputs of the noisy target with variance $\sigma^2 = 1$ are shown in Fig. 6c and d. It is obvious that the correlation peaks become lower and the correlation planes of Fig. 6c and d become less noisy compared to Fig. 4c and d. This occurs because the correlation of the low-contrast reference and the noise produces smaller output intensity than that of high-contrast image.

The 3D correlation outputs of the detection of the noise-free high-contrast fingerprint target pre-processed by the AMF with $N = 64.7\%$ and $N = 99.8\%$ are shown in Fig. 7a and b, respectively. Since the contrast ratio is greater than unity, the first correlation term of Eq. (7) produces higher correlation peaks than the autocorrelation outputs of the noise-free low-contrast target shown in Fig. 6. Following the preceding discussion, the differences of the peak intensities and the noise in the correlation plane between Fig. 7a and b are caused by the effect of the threshold. Fig. 7c and d show the correlation outputs of the noisy high-contrast target. Since the luminance value of the target image is higher than the noise, the desired correlation peak that is one order of magnitude lower than that of the noise-free case is still distinguishable. In this detection, the FAHM of the correlation signal does not change.

From the computation of the normalized PCDs for different targets detected by using the low-contrast fingerprint reference as a function of the percentage N, it is found that the resultant normalized PCDs are the same as the simulation results produced by using the high-contrast fingerprint reference. This occurs because of the same reason as discussed in Section 3.1. Besides having the same conclusion as the ones drawn in the preceding section, this result reveals that the performance of the modified AMJTC by using high-spatial-frequency reference images does not depend on the contrast of the reference, but is determined by the contrast of the target image and the noise present in the input plane.

3.3. High-contrast human face as the reference image

The autocorrelation outputs of the noise-free high-contrast human faces pre-processed by the AMF with $N = 96.3\%$ that corresponds to low threshold and $N = 99.9\%$ that corresponds to high threshold are illustrated in Fig. 8a and b, respectively. In comparison with the results of the fingerprint detection, the autocorrelation peak of the human face image is broader because the human face image contains less high-spatial-frequency components. By using the human face as the reference, the impulse response of the JTC becomes broader than that of the fingerprint reference [7]. As shown in Fig. 8a, the use of the AMF with low threshold gives sharper and lower correlation peak than that of Fig. 8b. This is the result of the edge enhancement of the AMF in which low-spatial-frequency components of the modified JPS are attenuated. Figs. 8c and d are the correlation outputs of the detection of the noisy high-contrast human face targets with variance $\sigma^2 = 1$ by using the AMF $N = 96.3\%$ and $N = 99.9\%$,

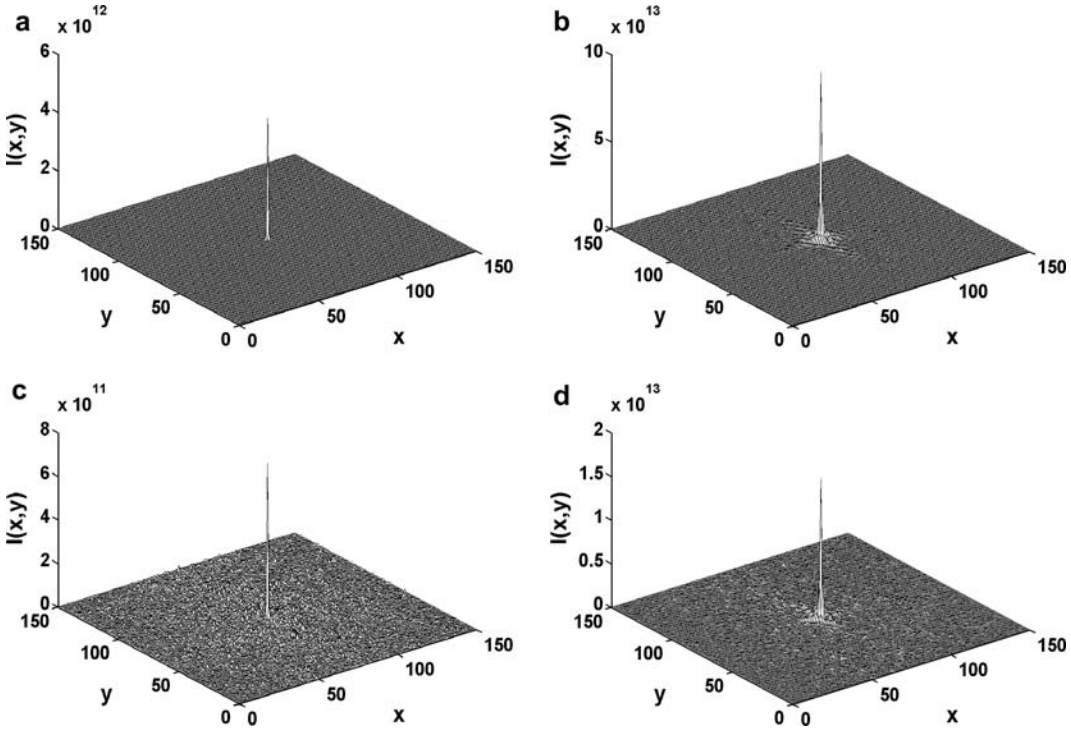

Fig. 7. Cross-correlation outputs of noise-free low-contrast fingerprint reference and noise-free high-contrast fingerprint target pre-processed by the AMF with (a) $N = 64.7\%$ and (b) $N = 99.8\%$. Cross-correlation outputs of noise-free low-contrast fingerprint reference and noisy high-contrast fingerprint target pre-processed by the AMF with (c) $N = 64.7\%$ and (d) $N = 99.8\%$.

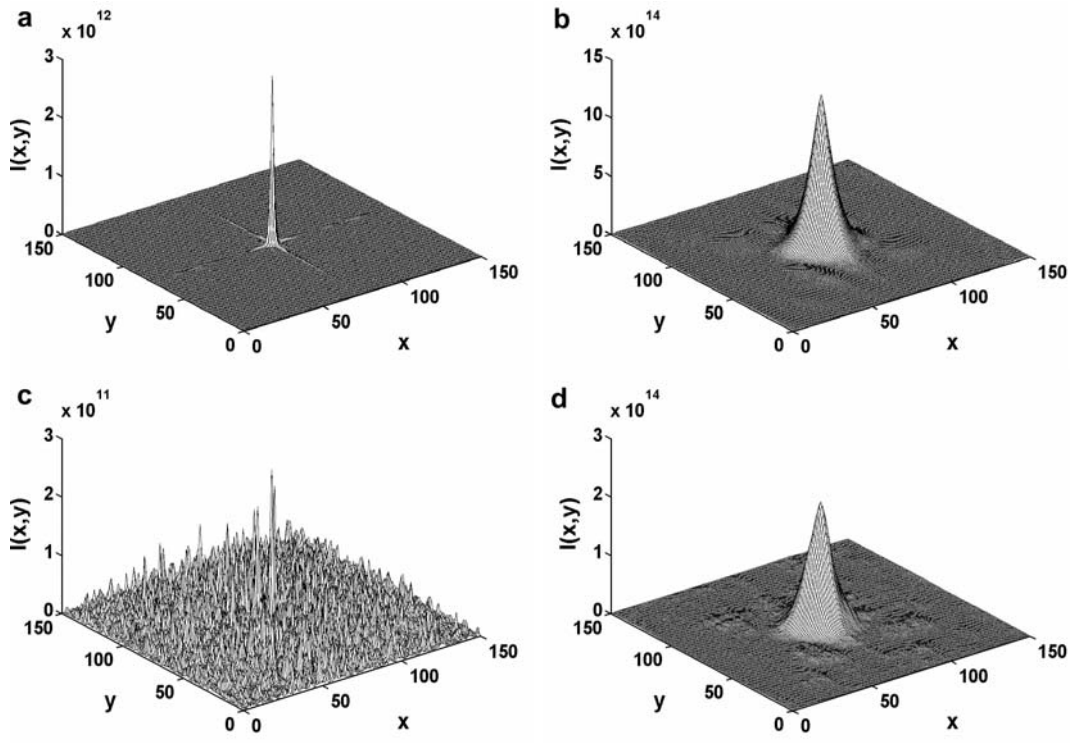

Fig. 8. Autocorrelation outputs of noise-free high-contrast human face pre-processed by the AMF with (a) $N = 96.3\%$ and (b) $N = 99.9\%$. Cross-correlation outputs of noise-free high-contrast human face reference and noisy high-contrast human face target pre-processed by the AMF with (c) $N = 96.3\%$ and (d) $N = 99.9\%$.

respectively. Although the preceding results show that the pre-processing of the JPS of the noisy target by using the AMF filter with high threshold gives noisy correlation output, the correlation planes of Fig. 8b and d do not appear to be noisy. This occurs because the noise components are smoothed out by the broad impulse response. However in the case of pre-processing by the AMF with low threshold, the edge enhancement effect sharpens the noise components.

Fig. 9a and b present the correlation outputs of the low-contrast human face detections obtained by using the AMF with $N = 96.3\%$ and $N = 99.9\%$, respectively. The widths of the correlation signals become as broad as Fig. 8a and b, while, their peak intensities are lower. This is because the target has a lower contrast compared to the reference. The desired correlation is scaled by the contrast ratio that is smaller than unity. Since the luminance of the low-contrast human face is smaller than the noise with variance $\sigma^2 = 1$, the detection of the corrupted low-contrast target produces noisy correlation plane as shown in Fig. 9c and d.

Fig. 10 shows the FAHMs of the modified AMJTC by using high-contrast human face reference as a function of the threshold percentage N for different targets. It is clear that the FAHMs depend on the percentage N. When the percentage number of pixels of the AMF with unity amplitude is 99.9%, the FAHMs of the noisy high- and low-contrast human faces are the broadest because they contain the summation of two broad correlation outputs. At the same percentage N, the FAHMs of the detection of different targets are smaller with almost the same values. When the percentage N becomes 99.2%, all the FAHMs fall sharply. This is mainly caused by the fact that the modified JPS contains narrow band of frequency components whose power decreases rapidly as the frequency becomes higher. Although the percentage N reduces slightly, most low-spatial-frequency components of the JPS is significantly attenuated. This sharpens the correlation peaks. As the percentage N reduces further, the FAHMs reduce slowly, because the variation of the power spectrum at higher spatial-frequencies is insignificant. The attenuation of these spatial-frequency components does not sharpen effectively the correlation peaks.

Fig. 11 shows the normalized PCDs as a function of the percentage N for different target scenes. For the same reason as discussed in the preceding sections, the normalized PCDs of the noise-free high- and low- contrast human face targets are the same. The normalized PCDs at $N = 99.9\%$ is 1.5, because the standard deviation of broad correlation width is much higher than that of the sharp ones. The normalized PCDs increase to be 10 as the percentage N reduces to 96.3%. Although their FAHMs are one order of magnitude greater than that of the noise-free fingerprint detection, the highest value of the normalized PCDs is higher than that of the fingerprint detection. This is because the value of the PCD of the human face detected by the classical JTC is smaller than that of the fingerprint. When the high-contrast human face target is corrupted by the noise, its normalized

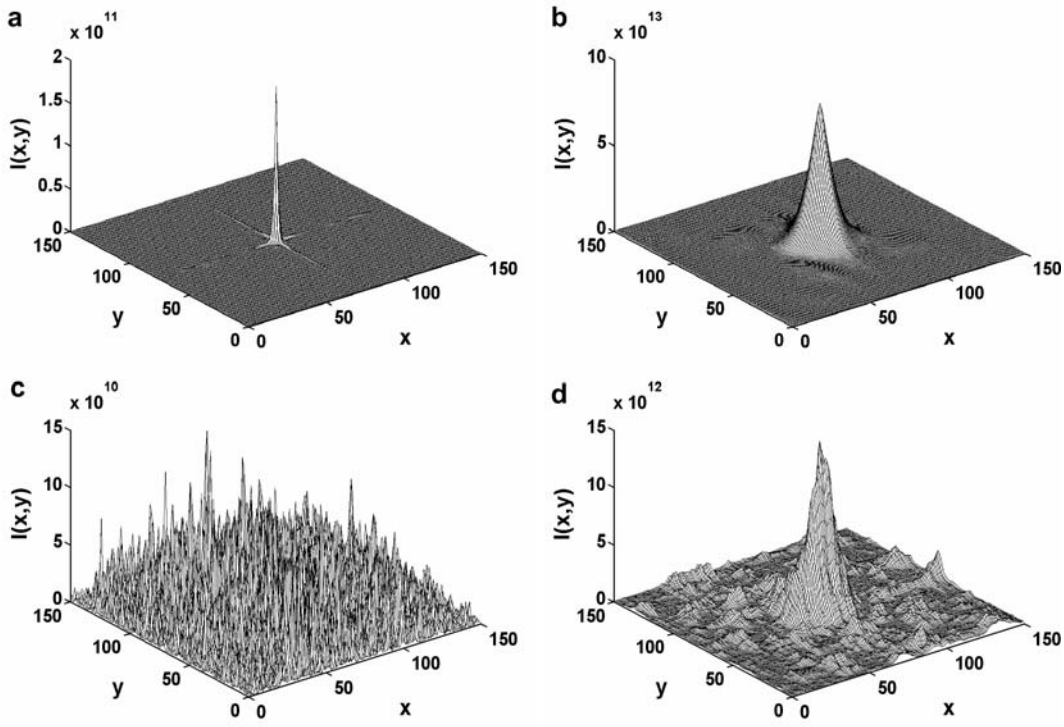

Fig. 9. Cross-correlation outputs of noise-free high-contrast human face reference and noise-free low-contrast human face target pre-processed by the AMF with (a) $N = 96.3\%$ and (b) $N = 99.9\%$. Cross-correlation outputs of noise-free high-contrast human face reference and noisy low-contrast human face target pre-processed by the AMF with (c) $N = 96.3\%$ and (d) $N = 99.9\%$.

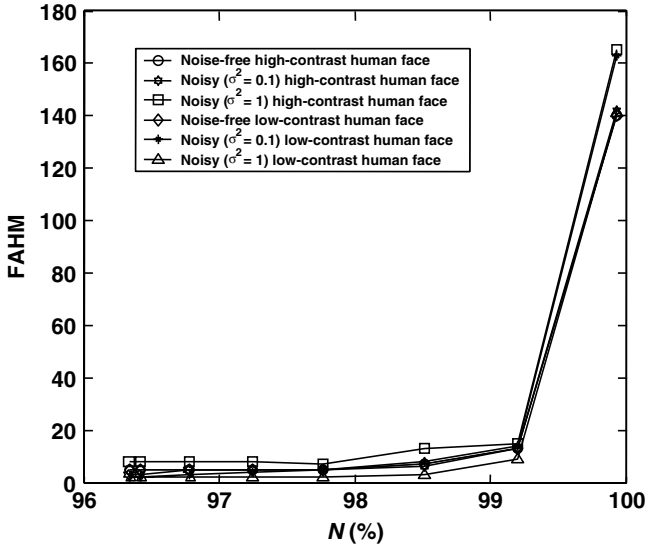

Fig. 10. The FAHM as a function of the percentage N of high-contrast human face reference.

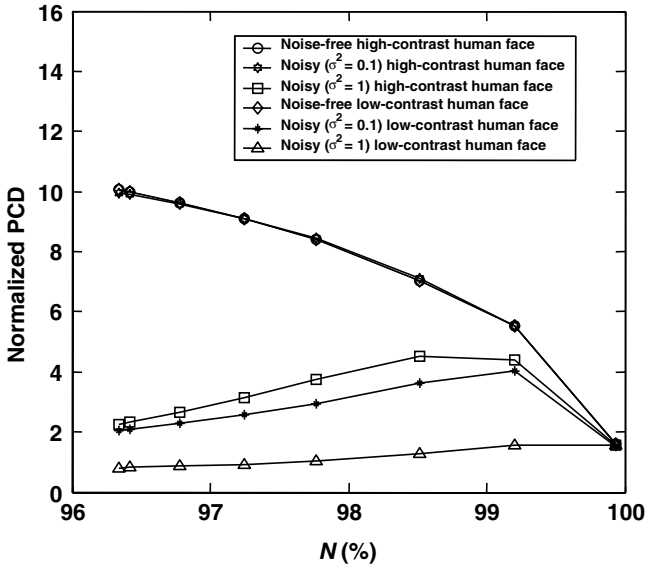

Fig. 11. The normalized PCD as a function of the percentage N of high-contrast human face reference.

PCD at highest percentage N is approximately equal to that of the noise-free detection results because the width of its correlation output is nearly the same. The raise of the normalized PCD to the highest value of 4.5 at $N = 98.5\%$ is followed by a gradual decrease as the percentage N becomes smaller. The high normalized PCD is obtained because the correlation output is sharpened such that the decrease in the standard deviation of the correlation intensity in the correlation plane is greater than that in the peak intensity. Since further decrease in the percentage N attenuates more spatial-frequency components of the JPS, the normalized PCD becomes lower. In the case of the detection of the noisy low-contrast human face target, the degradation of the performance of the modified AMJTC is more severe than the noisy high-contrast target. When the low-contrast

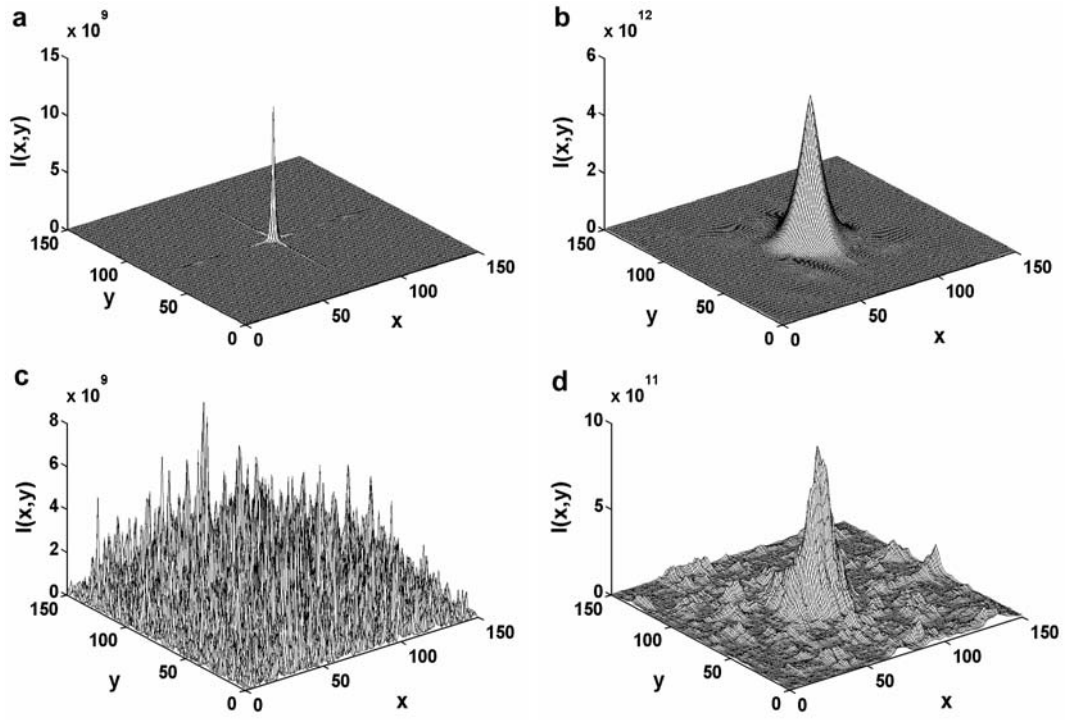

Fig. 12. Autocorrelation outputs of noise-free low-contrast human face pre-processed by the AMF with (a) $N = 96.3\%$ and (b) $N = 99.9\%$. Cross-correlation outputs of noise-free low-contrast human face reference and noisy low-contrast human face target pre-processed by the AMF with (c) $N = 96.3\%$ and (d) $N = 99.9\%$.

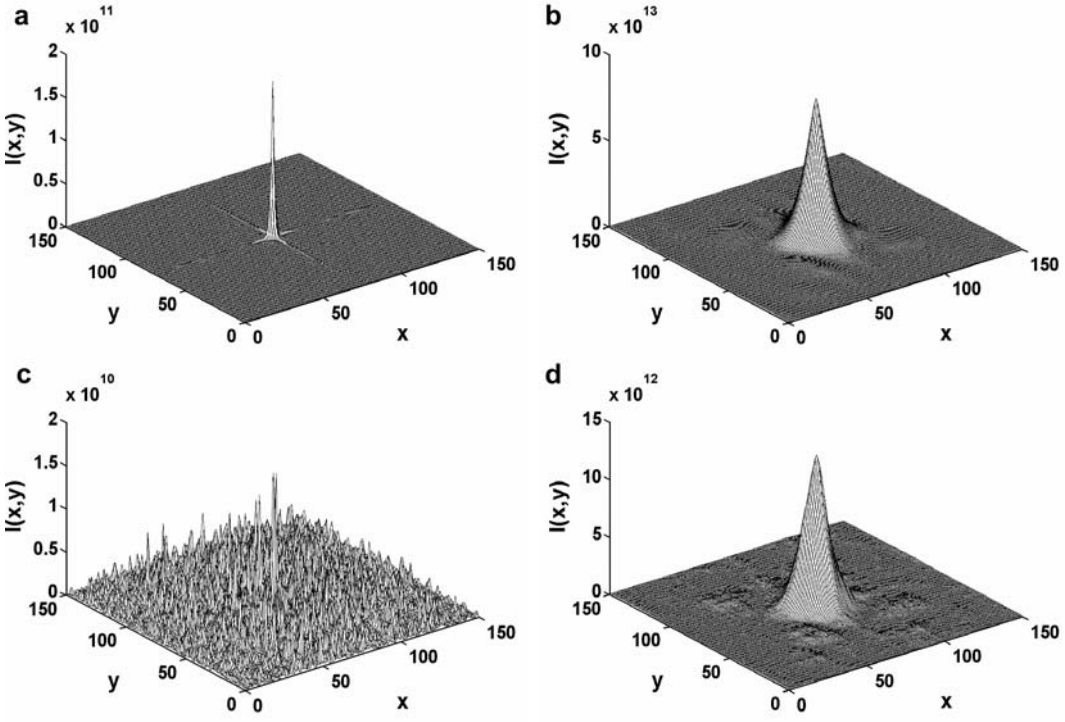

Fig. 13. Cross-correlation outputs of noise-free low-contrast human face reference and noise-free high-contrast human face target pre-processed by the AMF with (a) $N = 96.3\%$ and (b) $N = 99.9\%$. Cross-correlation outputs of noise-free low-contrast human face reference and noisy high-contrast human face target pre-processed by the AMF with (c) $N = 96.3\%$ and (d) $N = 99.9\%$.

Table 1
Optimization condition for the modified AMJTC

Reference images	Condition of target images			
	Noise-free		Noisy	
	High contrast	Low contrast	High contrast	Low contrast
High-contrast fingerprint	Low threshold	Low threshold	High threshold	None
Low-contrast fingerprint	Low threshold	Low threshold	High threshold	None
High-contrast human face	Low threshold	Low threshold	Intermediate threshold	Intermediate threshold
Low-contrast human face	Low threshold	Low threshold	Intermediate threshold	Intermediate threshold

human face target is corrupted by noise with variance $\sigma^2 = 1$, its normalized PCD is never higher than 1.6 regardless of the percentage N. Since it is caused by the presence of noise at the input, this detection performance is dependent upon the noise level.

In order to optimize the detection results, the suitable threshold of the AMF must be properly selected from appropriate values of the normalized PCD and the FAHM. For the noise-free targets, the AMF with low threshold should be used for detection because the resultant FAHM is the smallest and the normalized PCD is the highest. However, unlike the fingerprint targets, the detection of the noisy high-contrast human face cannot be done by using the AMF with high threshold. The appropriate threshold should be chosen from the sharp FAHM and the highest normalized PCD.

3.4. Low-contrast human face as the reference image

Fig. 12a and b show the 3D autocorrelation of the noise-free low-contrast human face target pre-processed by the AMF with $N = 96.3\%$ that corresponds to low threshold and $N = 99.9\%$ that corresponds to high threshold, respectively. Since the image contrast is low, the correlation peak intensities are lower by about three orders of magnitude than Fig. 8a and b. However, their widths are the same. The effect of using the AMF with low threshold which sharpens and reduces peak of the correlation intensity can be clearly seen from Fig. 12a. In the presence of strong noise with variance $\sigma^2 = 1$, the correlation outputs are degraded as shown in Fig. 12c and d. This is because the luminance of the low-contrast human face image is lower than the noise. According to Eq. (7), the second correlation term is greater than the first term. Therefore, the desired correlation peak illustrated in Fig. 12c is indistinguishable.

Fig. 13a and b shows the 3D correlation outputs of the noise-free high-contrast human face target pre-processed. Since the contrast of the target image is higher than that of the reference, the correlation peak intensities are higher than Fig. 12a and b. For this reason, the correlation peak can be observed from Fig. 13c although the input target is corrupted by strong noise.

For the same reason as discussed in Section 3.2, the FAHMs and the normalized PCDs of the modified AMJTC by using low-contrast human face reference are the same as the results of the high-contrast reference.

4. Conclusions

We have investigated quantitatively the effects of threshold on detection performance of the modified AMJTC by using the PCD and the FAHM. In this study, fingerprint and human face images were used as test scenes in the presence of noise and the contrast difference between the target and the reference that may rise from unbalanced illumination.

Of the four types of reference images, the normalized PCD of the human face detection is greater than that of the fingerprint. This is because broad correlation peak produced by the classical JTC yields smaller value of the PCD of the human face detection compared to the fingerprint. When the PCD of the human face detected by the modified AMJTC is normalized by the resultant classical PCD, its normalized PCD becomes larger than that of the fingerprint. By taking the value of normalized PCDs into account, the simulation results show that the detection of human face can be improved greater than that of fingerprint. The effects of threshold on single-target detection depend on the noise level in the input, the contrast and the spatial-frequency content of the target. When the target is low-contrast image with high-spatial frequency content, the modified AMJTC is not tolerant to noise. Table 1 summarizes the optimization condition for the modified AMJTC. It can be concluded from this table that the detection performance can be optimized by selecting appropriate threshold value, which depends on the noise level in the input, the contrast and the spatial-frequency content of the target.

Acknowledgements

The financial support from Thailand Research Fund through the Royal Golden Jubilee Ph.D. Program (Grant No. PHD/0020/2547) is acknowledged.

References

[1] M.S. Alam, M.A. Karim, Opt. Eng. 33 (1994) 1610.
[2] R.K. Wang, L. Shang, C.R. Chatwin, Appl. Opt. 35 (1996) 286.
[3] X. Huang, H. Lai, Z. Gao, Appl. Opt. 36 (1997) 9198.
[4] M.S. Alam, M.A. Karim, Appl. Opt. 32 (1993) 4344.
[5] M.S. Alam, M.A. Karim, Proc. IEEE (1993) 1074.
[6] D. Feng, H. Zhao, S. Xia, Opt. Commun. 35 (1991) 260.
[7] J. Widjaja, U. Suripon, Opt. Eng. 43 (2004) 1737.
[8] D. Roberge, Y. Sheng, Opt. Eng. 33 (1994) 2290.
[9] J. Widjaja, U. Suripon, Opt. Commun. 253 (2005) 44.